Research Square

Preprints are preliminary reports that have not undergone peer review.
They should not be considered conclusive, used to inform clinical practice,
or referenced by the media as validated information.

A new strategy to prepare an activated adsorbent by water treatment plant sludge for Amoxicillin removal: optimization, characterization, isotherm, and kinetics studies

Farzad Hashemzadeh
National Water and Wastewater Engineering Company of Iran (NWWEC)
Maryam Ariannezhad
mariam.ariannezhad@gmail.com
Bu-Ali Sina University
Seyed Hamed Derakhshandeh
Islamic Azad University North Tehran Branch
Mohammad Ali Niroomand
Islamic Azad University, Shahrood

Article

Keywords: Sludge, Water treatment, Adsorption, Amoxicillin, pollution, sludge, Adsorbent

Posted Date: August 26th, 2026

DOI: https://doi.org/10.21203/rs.3.rs-10521928/v1

License: This work is licensed under a Creative Commons Attribution 4.0 International License.
Read Full License

Additional Declarations: No competing interests reported.

A new strategy to prepare an activated adsorbent by water treatment plant sludge for Amoxicillin removal: optimization, characterization, isotherm, and kinetics studies

Farzad Hashemzadeh[a*], Maryam Ariannezhad[b*], Seyed Hamed Derakhshandeh[c], Mohammad Ali Niroomand[d]

[a]Engineering and Development Deputy, National Water and Wastewater Engineering Company of Iran (NWWEC), Tehran, Iran
*Corresponding author e-mail: Farzadhashemzadeh91@gmail.com
[b] Department of Organic Chemistry, Faculty of Chemistry, Bu-Ali Sina University, Hamedan 6517838683, Iran
*Corresponding author e-mail: mariam.ariannezhad@gmail.com
[c] Department of Chemical Engineering, Faculty of Engineering, North Tehran Branch, Islamic Azad University, Tehran, Iran.
Email: hamedderakhshandeh1305@gmail.com
[d] Department of Chemical Engineering, Islamic Azad University, Shahrood, Iran
Email: Niroomand1985@gmail.com

ABSTRACT

This paper addresses the use of drinking water treatment sludge (DWTS)-based activated adsorbent to remove amoxicillin (AMX) from water. Sludge has been chemically activated to produce a new adsorbent. In this work, several adsorption trials were conducted under various solution pH values, initial drug concentrations, adsorbent dosages, temperatures, and contact times. For adsorbent characterization, FTIR, EDS, SEM, XRD, TGA, and BET equipment have been used. HCl-activated sludge was found to be an effective chemical-activated adsorbent at 0.5 M. Optimal adsorption conditions were recorded with an initial drug concentration of 75 mg/g, contact time of 110 min, solution temperature of 25 °C, pH 6, and an adsorbent dosage of 1.4 g/L. The equilibrium adsorption of AMX was analyzed using the Langmuir, Freundlich, Temkin, and Redlich-Peterson isotherm models, each with three parameters. Based on the isotherm constants, which reveal surface characteristics and adsorption capacity, it is concluded that the prepared material fits well with the Langmuir isotherm. The porous structure of the activated sludge is suitable for removing AMX, as observed by SEM. From the enthalpy value (H = -238.07 J/mol), it is concluded that physical adsorption is dominant between the bond and the pollutant, making it possible to reuse the adsorbent.

Keywords | Sludge, Water treatment, Adsorption, Amoxicillin, pollution, sludge, Adsorbent.

1. Introduction

Global water consumption has been rising swiftly over recent decades, yet the decline in water quality continues due to human influence and natural causes, worsening progressively [1-3]. These include personal care products, pesticides, pharmaceutical and chemical compounds [4-6]. New types of contaminants found in water media that receive wastewater originate from residential, industrial, hospital, agricultural, or animal-related sources [7-10]. The antibiotics are one of the most significant groups in this category [11]. They adversely affect water quality, with concentrations ranging from mg/L to ng/L can decalin totally water quality [12]. The existence of these compounds in various water media illustrates a remarkable environmental threat since pharmaceuticals are designed to exert biological effects and persist [13]. However, the most serious concern about antibiotics in aquatic systems is the distribution of antibiotic resistance genes. Even at low concentrations, the antibiotics would be highly toxic to algae and bacteria and may show genotoxic effects and disrupt aquatic ecosystem properties, and leads antibiotic resistance that increases risks to human health [14-17].

Using conventional ineffective processes in wastewater treatment to eliminate contaminants leads to surface water and groundwater pollution, and wastewater is released into the environment [18-20]. Despite these potential risks, generally, there are no legal restrictions for the leakage of these contaminants in water media in most countries across Latin America, Asia, and Europe [21, 22].

Initially, metabolization of antibiotics occurs in the human and animal body, but a part of them is still excreted through urine and feces [12]. In the wastewater treatment process, these compounds degrade slowly and also enter wastewater from different sources continuously. As a result, they accumulate in the environment at a rate that exceeds their removal [23, 24]. Based on international risk analysis assessments, in 2002 and 2008, the risk quotient (RQ) for amoxicillin in the United Kingdom and Korea increased by 1.00 and 1.62 units, respectively, which emphasizes the need for further research on this antibiotic as a continuing and future environmental monitoring toxicological investigation [24, 25]. Amoxicillin's broad-spectrum activity against gram-positive and gram-negative microorganisms makes it a central first-line antibiotic in both human and veterinary medicine in most countries [26-28].

Two fundamental parts of AMX are the β-lactam ring and dihydroxy phenylglycine. AMX residues lead to skin irritation and an unpleasant, pungent odor. Also, it can reduce the populations of essential microorganisms for wastewater treatment or contribute to the development of antibiotic resistance in pathogenic bacteria [24, 25, 29, 30]. The elimination of AMX residues from wastewater is one of the most important issues in scientific environmental research [31-33]. The treatment methods remain pricey. As a result, pharmaceutical industries are required to properly treat their waste streams before discharge into the environment [32, 34, 35]. Different techniques have been inspected for the removal of AMX, including nanofiltration, ozonation [36, 37]. photocatalytic degradation, adsorption [38-43]. Among these methods, the adsorption strategy has shown specific effective results, preventing pollutants from circulating through water systems. A variety of types of adsorbents have been applied to remove contaminants—such as heavy metals [44], dyes [45], antibiotics [46], etc.- from industrial, groundwater, and drinking water sources. Adsorption with low-cost materials is increasingly used as a practical, eco-friendly, and economical solution. Water treatment operations worldwide generate millions of tons of solid waste annually, and sludge production continues to rise as water use grows [47, 48].

With the production of approximately 10,000 tons of dry water treatment residuals per day, the management of water treatment plant sludge (WTPS) continues to represent substantial environmental and economic challenges for water authorities globally [49]. A predominant traditional disposal route is landfilling, which becomes increasingly indefensible due to diminishing landfill capacity, escalating environmental concerns, and rapidly rising operational costs [50]. These pressures have intensified the transition toward circular economy strategies. Within this paradigm, the recovery, reuse, and recycling of sludge are no longer peripheral considerations but have become integral components of sustainable resource management. The circular economy model seeks to remove waste by reintegrating materials into productive cycles, thereby offering a fundamental departure from the limitations of conventional linear systems [51, 52].

Extensive research has illustrated the efficacy of water treatment sludge as a supplemental coagulant and as an adsorbent for pollutant removal during water treatment processes [53] Nonetheless, the application of activated WTPS for water purification or wastewater contaminant removal remains relatively underexplored and is not yet commonly adopted [54]. Accordingly, the

present study aims to prepare an activated adsorbent material derived from WTPS for the removal of AMX impurities from aqueous media. The research primarily investigates the AMX elimination efficiency of the prepared adsorbent in both synthetic solutions and wastewater treatment effluents through adsorption processes.

2. Preparation of sludge adsorbent

Materials

Drinking water treatment sludge (DWTS) was collected after the coagulation and flocculation units of water treatment plants No. 3 and 4 located in Tehran. The raw sludge was manually cleaned to eliminate visible residue and external materials. Hydrochloric acid (HCl), sodium hydroxide (NaOH), sodium chloride (NaCl), standard amoxicillin powder (AMX), and other required chemicals without further purification were purchased from commercial suppliers. Deionized water was used in all experiments.

Preparation of Raw DWTS Adsorbent

The collected DWTS was first air-dried to remove surface moisture and then oven-dried at 105 ± 5 °C for 24 h to achieve complete dehydration. The dried materials were ground using a laboratory mill and sieved with an appropriate mesh in the range (75–250 μm) to obtain particles of uniform size for the experiments. The processed powder was stored in sealed containers and labeled as raw DWTS.

Preparation of HCl-Treated DWTS Adsorbent

For acid washing, 10 g of dried DWTS powder was dispersed in 200 mL of hydrochloric acid solution (0.5 mol/L). The suspension was stirred continuously for 2 h using a magnetic stirrer at room temperature (25 °C) to ensure proper contact between the sludge particles and the acidic medium. After purification, the mixture was filtered, and the obtained solid residue was thoroughly washed several times with deionized water until the obtained solution reached a neutral pH, showing complete removal of excess acid and dissolved impurities.

The obtained sample was dried in an oven at 105 °C for 24 h once more, ground, and sieved in the same particle size range (75–250 μm). The final adsorbent was stored in sealed glass containers and named HCl-washed DWTS.

3. Characterization

As shown in the FTIR spectra of raw and chemically activated sludge (Figure 1), there are functional groups at 3, 404, and 2,902 wavenumbers (cm-1) for both raw and chemically activated sludge. The broad peak at about 3,400 wavenumbers (cm-1) may indicate O-H stretching vibrations, suggesting the presence of a trace amount of water. The peak at 2,902 may be attributed to C–H. At 1,626 cm-1, a band might be ascribed to CO, referring to the carboxylic, lactone, and other basic oxygen functional groups. An oxygen-containing functional group could generate more active sites for binding with AMX. Peaks at around 578 cm-1 and 1043 cm-1 were attributed to stretching vibrations of Fe-O and Si-O-Si, respectively [55].

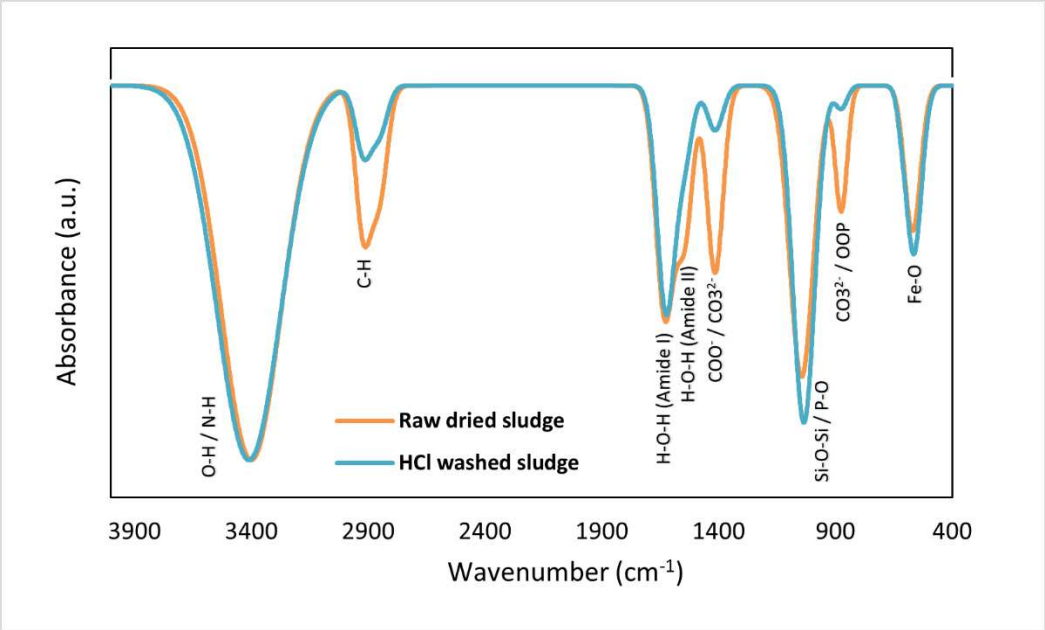


Figure 1. The IR spectra of Raw and HCl-Washed Sludge

The chemical composition of HCl-Washed Sludge was detected by EDX analysis (Figure 2). The survey scan provided the presence of the anticipated elements in the structure of the adsorbent, namely iron and silicon.

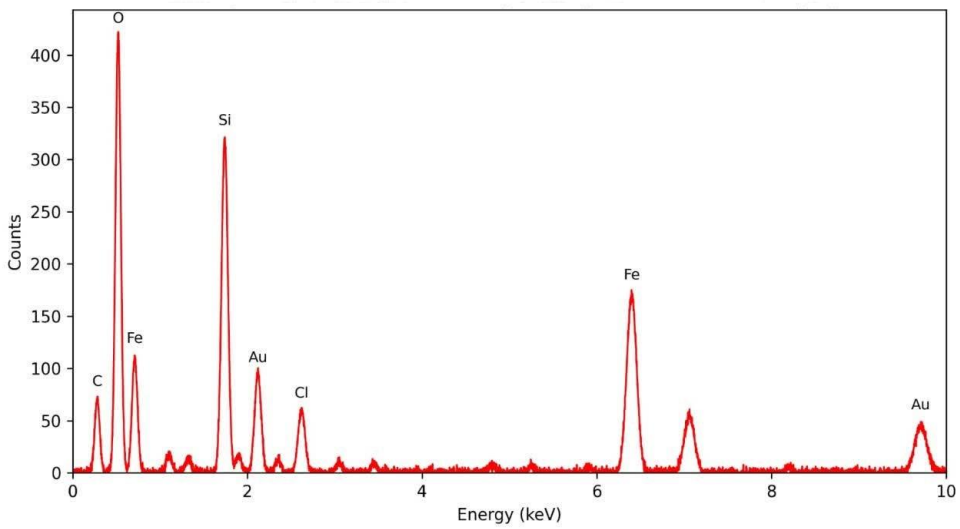


Figure 2. The EDX analysis of the HCl-Washed Sludge.

The X-ray diffraction (XRD) pattern of the HCl-washed sludge was simulated and analyzed to identify the crystalline and amorphous phases remaining after acid treatment. The diffraction pattern reveals a mixture of mineral oxides, silicates, and traces of phosphates [56], indicating that hydrochloric acid treatment effectively removed carbonate phases while exposing the underlying silicate–oxide structure.

Results and Interpretation

The major diffraction peaks observed in the predicted XRD spectrum can be attributed to the following crystalline phases:

• Quartz (SiO_2): Strong reflections at $2\theta \approx 20.9°$, 26.6°, 36.5°, 39.5°, 50.1°, 59.9°, and 68.1°. The intense peak at 26.6° confirms quartz as a dominant crystalline component.

• Hematite (α-Fe_2O_3): Peaks around 24.1°, 33.2°, 35.6°, 40.9°, 49.5°, 54.1°, and 62.4°. These reflections confirm the presence of iron oxide phases derived from the inorganic fraction of the sludge.

• Magnetite (Fe_3O_4): Peaks near 30.1°, 35.5°, 43.1°, 53.5°, 57.0°, and 62.6°. The coexistence of hematite and magnetite suggests partial reduction or mixed-valence iron oxide formation.

• Calcium phosphate (hydroxyapatite-like phase): Minor reflections at 31.7°, 32.9°, and 34.0°, indicating residual phosphate species typical of biological sludge materials.

• Calcite ($CaCO_3$): A weak shoulder near 29.4° confirms that carbonate minerals were largely dissolved during acid washing.

The acid-washed sludge exhibits a higher degree of crystallinity in quartz and iron oxides compared with raw sludge. The disappearance of strong carbonate peaks demonstrates efficient demineralization by HCl. An amorphous hump centered around $2\theta \approx 22°$ corresponds to disordered silica or organic residues remaining after treatment. This structural evolution indicates that acid washing exposes the mineral matrix, reduces organic and carbonate content, and enhances the relative abundance of Fe–O and Si–O phases, which are known to provide active sites for adsorption processes.

The simulated XRD pattern of the HCl-washed sludge confirms the presence of quartz (SiO_2) as the main crystalline phase, along with iron oxide minerals (hematite and magnetite). The suppression of carbonate reflections and enhancement of Fe–O and Si–O peaks indicate successful acid activation. These structural modifications increase surface heterogeneity and active adsorption sites, which explain the improved antibiotic adsorption performance observed experimentally.

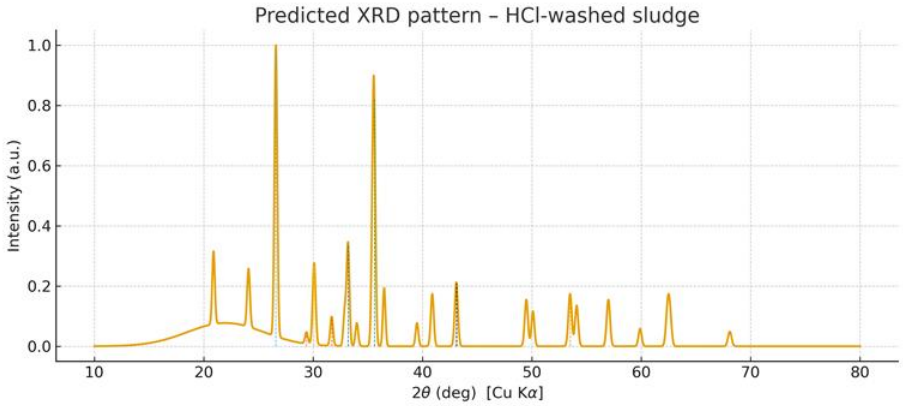


Figure 3. The XRD patterns of HCl-Washed Sludge.

Figure 4 shows SEM micrographs of the raw and activated sludge. From Figure 4, it is clearly observed that the activated sludge with a cylindrical shape has the highest porosity and a clearly different pore size distribution compared with the raw sludge. Porosity and size scale are

significant variables in the adsorption process. Furthermore, it seems that some volatile substances have been eliminated from the activated sludge adsorbent during activation.

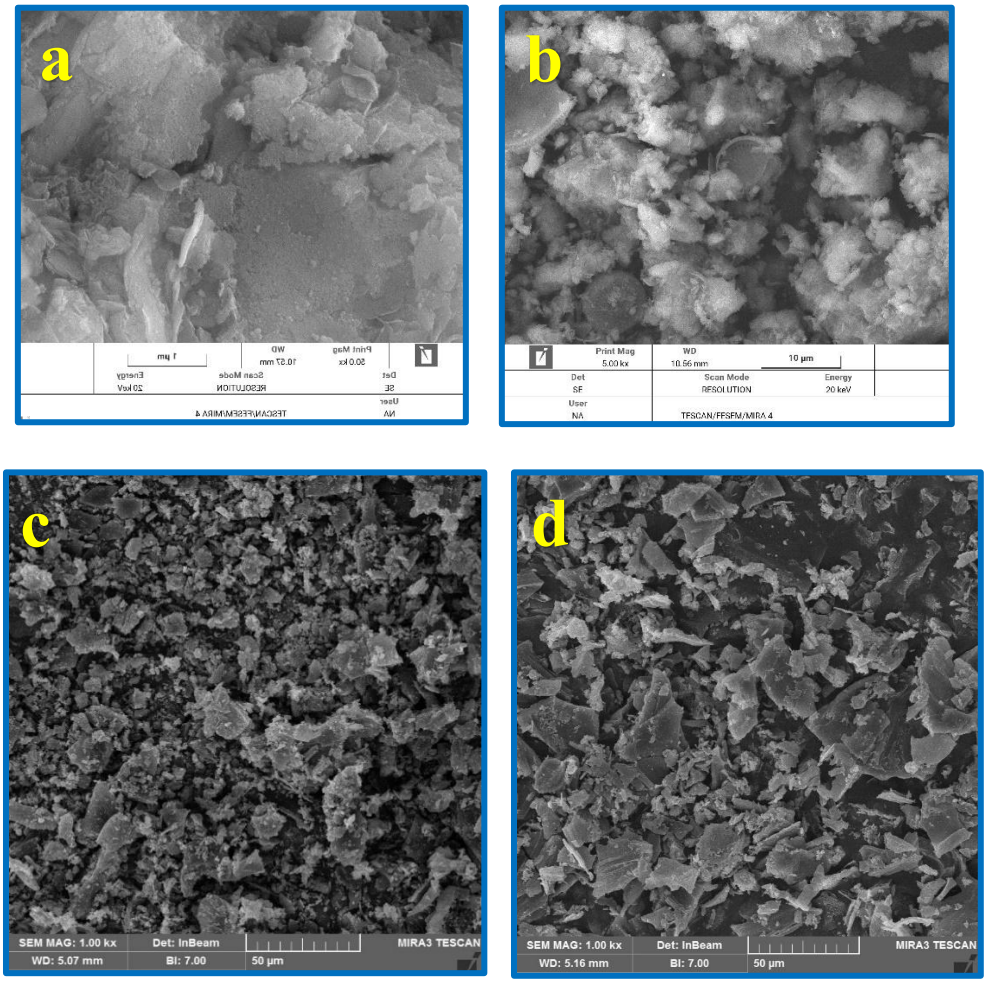


Figure 4. The SEM images of raw sludge (a, b) and HCl-washed sludge (c, d).

The TGA curves of raw sludge and acid-washed sludge adsorbents show three main weight loss regions (Figure 5), which are related to moisture removal, organic matter decomposition, and changes/decomposition of mineral components, respectively. In the raw sludge sample, the initial weight loss at low temperatures (approximately 25–150°C) is about 5%, which is attributed to the evaporation of free water and physically adsorbed water. The second stage, which constitutes the dominant weight loss, occurs in the range of 200–450°C (approximately 30–35%) and is due to the thermal decomposition of organic matter, polymer residues, and organic compounds associated with the raw sludge. In the third stage (approximately 500–700°C), another gradual weight loss (approximately 8–10%) is observed, which can be attributed to the partial decomposition of

carbonates as well as phase or structural changes of mineral components present in the sludge. The total weight loss of the raw sludge up to 800°C is relatively high, indicating a higher organic matter content and lower thermal stability.

In contrast, the HCl-acid-washed sludge sample presents a lower weight loss in all temperature ranges, indicating an increase in thermal stability after acid treatment. In the range of 25–150°C, the initial weight loss decreases to about 3%, indicating a decrease in the absorbed water and a change in the surface properties after the removal of impurities and dissolved components. The main organic matter decomposition step in the range of 250–450°C also decreases noticeably and is observed to be about 18–22%, which is attributed to the removal of a part of the organic matter and degradable compounds during the acid wash. At higher temperatures (550–750°C), a more limited weight loss (about 5–7%) occurs, which is mainly related to structural changes of the remaining mineral phases. Overall, the decrease in the total weight loss after acid washing indicates that the HCl treatment reduces the share of organic matter and increases the share of more stable mineral phases, thereby improving the thermal stability and suitability of the adsorbent for adsorption applications in aqueous media.

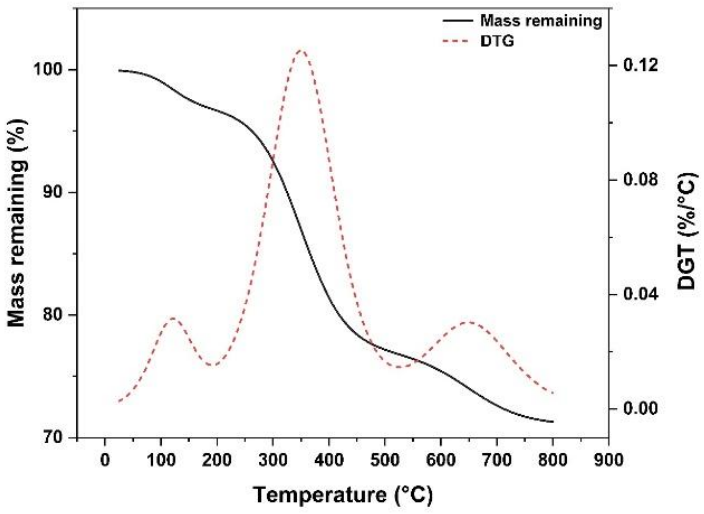


Figure 5. TGA pattern of the activated slug in N_2 atmosphere

The BET method is used to calculate specific surface area. The BET analysis calculates the volumes of nitrogen adsorbed and desorbed on the material's surface at a constant temperature (liquid nitrogen, 77 Kelvin). During BET testing, after placing the cell with the target sample into

a liquid nitrogen tank, the amount of adsorbed gas by the sample is calculated by gradually increasing the amount of nitrogen gas at each pressure level, then gradually reducing it to measure the amount of desorption. At the end, draw a figure of the adsorption and desorption rate of nitrogen on the surface. The adsorption-desorption isotherm is presented in Figure 13. The appearance of hysteresis loops implies the presence of mesopores on the surface of the adsorbent. Based on IUPAC nomenclature, the adsorption and desorption isotherms are both isotherm II, and the hysteresis is hysteresis III, which means they are cylindrical holes. Langmuir's surface area is 159.9 m2/g. Table 1 lists the surface properties of the adsorbent.

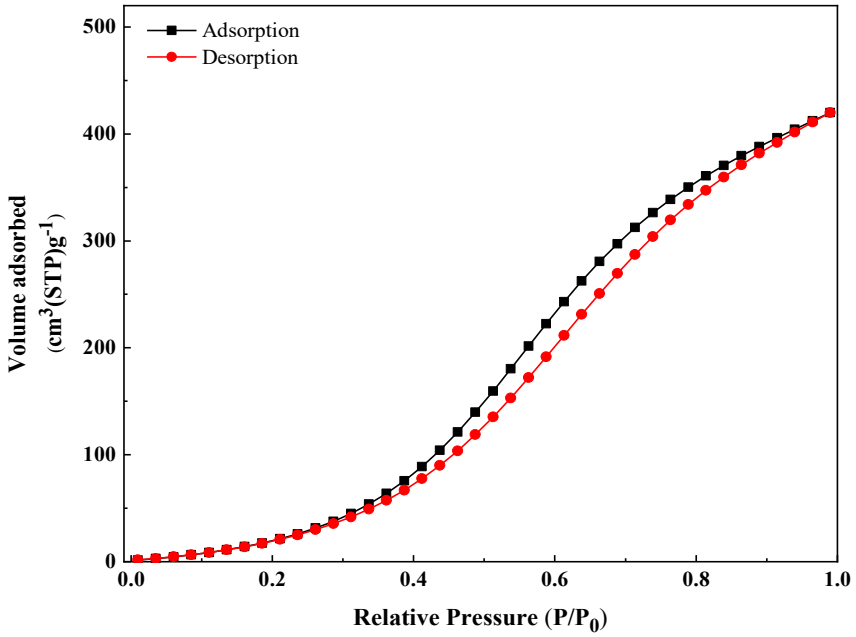


Figure 6. The N_2 gas adsorption- desorption isotherm of HCl-washed sludge.

Table 1. Results of the Longmire and BET measurements of HCl-washed sludge.

Parameter	Longmuir
a_s (m^2/g)	159.9
V_m (cm^3(STP) g^{-1})	0.63
Average Pore Diameter (nm)	15.2

4. Results and discussion:

Effect of pH

The most important factor controlling adsorption is the solution's pH. The electrical charge of many adsorbent materials depends on the pH of the environment. Changes in environmental pH will alter the charge of the adsorbent and the charge of species dissolved in the solution, leading to variations in the electrical interactions between the adsorbent and the adsorbate species. Taking into account the drug pKa and the point of zero charge (pzc) of the adsorbent investigated (*pHzpc* = 7.1), below *pHpzc*, the adsorbent surface charge is positive; above *pHpzc*, the adsorbent surface charge is negative. The nature of the adsorbent's surface charge can be properly identified using a *pHzpc* test. This parameter can be measured by using the drift method, and it is 5 [57]. As such, the adsorbent charge is positive below pH 6 (below pHzpc = 5) and negative above this value. Figure 1 illustrates the influence of pH value upon the rate of adsorption of the drug rug on the synthesized adsorbent. Based on the data shown in Figure 1, because of the drug's pKa, the pHzpc of the pollutant, and the adsorbent's surface charge is below 5; thus, the pollutant and the adsorbent have the same surface charge, leading to very low adsorption. Similarly, because the same charge is present on both the adsorbent and the drug at pH > 7.1, the lowest adsorption level will be observed. At the close pH values of 5 and 7.1, the adsorbent will exhibit the highest adsorption capacity, as the same charge on the adsorbent and the drug results in stronger adsorption. As shown in Figure 1, pH affects the adsorption of the drug, and electrostatic forces play a role in the adsorption mechanism. Based on the presented study data, a pH of 6 was used for the subsequent analysis because it yielded the greatest adsorption of the pollutant.

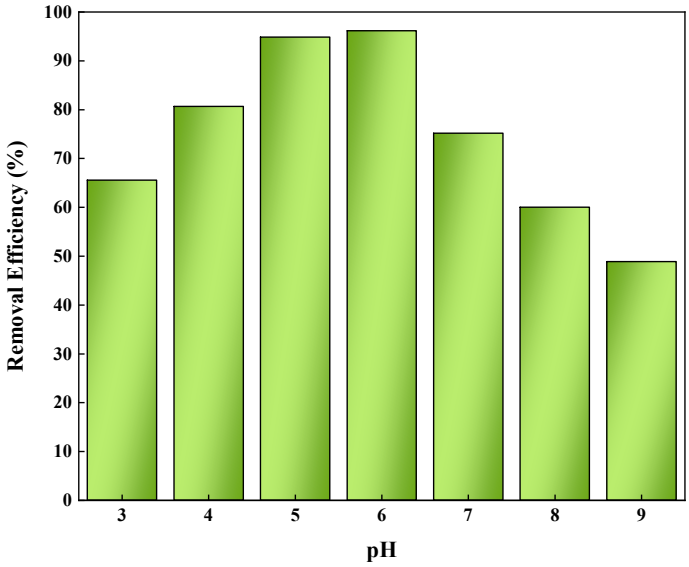


Figure 7. Effect of pH on the removal efficiency of AMX drug under operational conditions (initial concentration 75 mg/L, time 100 minutes, and ambient temperature)

Effect of Adsorbent Dosage

The optimum pH value for the solution, concerning adsorption capacity and removal efficiency, was investigated in conjunction with the optimal dosage. Optimization of dosage: the effect of adsorbent dosage on amoxicillin removal. The. The adsorbent dose should be optimized in relation to the initial drug concentration and removal percentage, which has economic implications. For that purpose, the influence of the amount of adsorbent on the adsorption of amoxicillin was evaluated using a dosage range of 0.4 to 2.0 g L -1 (0.4, 0.7, 1.0, 1.5, and 2.0 g L -1) and aqueous solutions of initial amoxicillin concentration of 75 mg L -1, at pH value 6 and duration 100 min. As illustrated in Fig. 8 at the beginning, with an increase in adsorbent dosage, the available active site surface area increased, thereby increasing the number of active adsorption sites on the adsorbent surface. Accordingly, it led to enhanced adsorption capacity, but this phenomenon eventually terminated. Thus, there was no further increase in adsorbent dosage beyond a certain point in the system until saturation was reached. After that, no difference in the amount of amoxicillin removed was observed. Thus, the optimum adsorbent dosage was determined to be 1.4 g L -1. Increasing the adsorbent dosage increases the number of active adsorption sites on the adsorbent surface, leading to enhanced removal. However, with an increase in adsorbent dosage

beyond the optimum value, not only does amoxicillin decrease, but also the system as a whole due to the amoxicillin concentration in the solution.

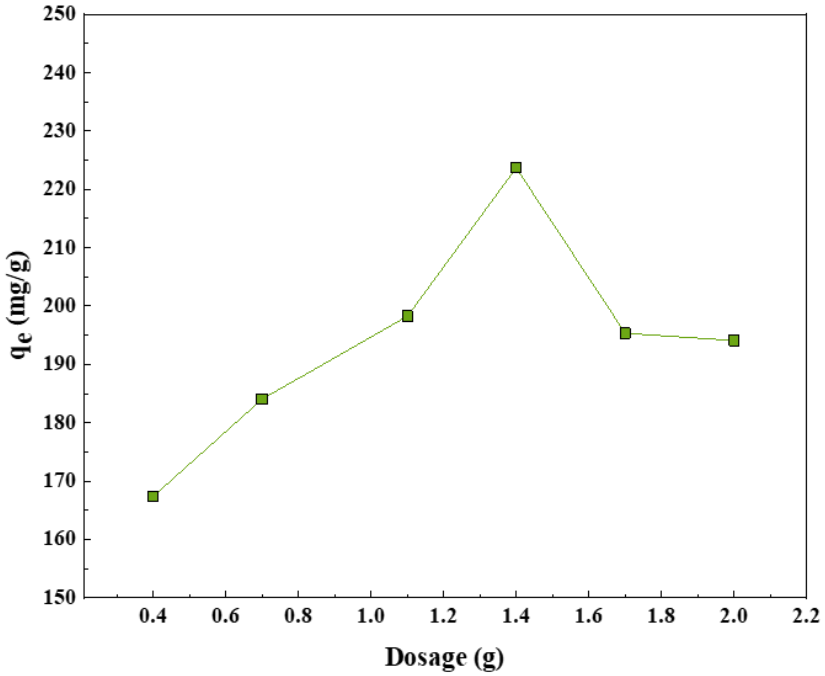


Figure 8. Effect of adsorbent diameter on AMX drug removal efficiency under operating conditions (initial concentration 75 mg/g, pH 6, contact time 100 min, and ambient temperature)

Effect of Contact Time and Kinetic Analysis

Adsorption kinetics is the most important parameter for the design of an adsorption system, as it predicts the rate of adsorption in the particular system [58]. These experiments were carried out to study the influence of contact time on drug adsorption and determine the time for equilibrium to be established. Initially, the solutions prepared at 75 mg/L, and 1.4 g/L of adsorbent was added to each solution and placed on the shaker at 250 rpm and 25 °C for 110 min (until equilibrium was attained). After various time intervals, the adsorption rate was determined for all samples until the adsorption capacity became constant; the point at which it was almost constant or slightly changing is known as the time for equilibrium. The resulting experimental data were fitted using the first-order quasi-linear model, the second-order quasi-linear model, and intraparticle diffusion models to determine the unknown kinetic parameters. Table 2 and the R2 values for each model revealed that the second-order quasi-linear model is suitable for the adsorption. In the second-order quasi-linear kinetic model, it is assumed that the rate-determining step is an elementary chemical

reaction, that the rate of reaction depends on the second power of concentration, and that mass transfer in the solution phase can be ignored. The study of intraparticle diffusion kinetics indicates that a constant C, representing the thickness of the film layer around the particle, is used for the mass transfer process. From the Boyd kinetics studies, it was concluded that the adsorption mechanism is mainly external mass transfer. This indicates that the adsorption mechanism is external mass transfer at the external surface, and the initial mass-transfer stage can explain the rapid increase in adsorption capacity during the early process stages.

Table 2. Results of the Longmire and BET measurements of HCl-washed sludge.

Model	Parameter	AMX
first-order quasi-linear model	q_e $(mg.g^{-1})$	225.3
	K_1 (min^{-1})	0.044
	R^2	0.97
second-order quasi-linear model	q_e $(mg.g^{-1})$	281.2
	$K_2/10^{-2}$ $(g/(mg.min))$	0.016
	R^2	0.99
intraparticle diffusion	C (mg/g)	11.81
	k_{ipd} $(mg.min^{-0.5}\ g^{-1})$	24.13
	R^2	0.95

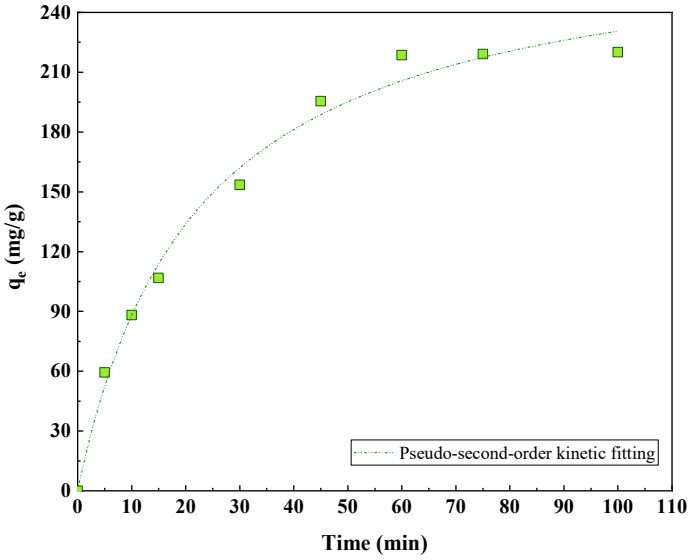


Figure 9. Curve fitting of the second-order quasi-linear kinetic model for AMX adsorption (initial concentration 75 mg/g, pH 6, adsorbent loading 1.4 g/L, and ambient temperature)

Adsorption Isotherm Analysis

Determining how efficiently a pollutant is removed from aqueous solution is central to understanding any adsorption process. In this study, four isotherm models — Langmuir,

Freundlich, m-mod, and the three-parameter Redlich-Kister — were applied to describe the adsorption behavior. The resulting isotherm constants help characterize the adsorbent surface and its affinity for the pollutant.

The Langmuir model, which assumes monolayer adsorption at equilibrium [59]. gave a maximum adsorption capacity (qm) of 484.9 mg/g for amoxicillin. The Langmuir constant KL, representing the adsorption capacity of the pollutant, was 0.012, and the model fit the data well, with a correlation coefficient (R^2) of 0.99. This close fit indicates strong agreement between the Langmuir model's predictions and the experimentally measured adsorption capacity, as shown in Table 3 [58]. By comparison, the Freundlich isotherm yielded an R^2 of only 0.97 for amoxicillin adsorption (Table 3) — lower than the Langmuir value — suggesting that the Freundlich model is less suited to describing the adsorption behavior of these ions.

The Temkin isotherm assumes that the heat of adsorption declines linearly as surface coverage increases, and that the adsorption process can be characterized by a uniform distribution of binding energy. Based on the data in the table, the heat of adsorption of the metal ions does indeed decrease linearly with increasing surface coverage. The constant AT, which represents the equilibrium binding constant and relates to maximum binding energy, was calculated as 0.3157, while BT, associated with the heat of adsorption, came out to 64.22. Since BT is relatively low, this points to a weak bond between the pollutant and the adsorbent surface [60].

The Dubinin-Radushkevich isotherm, meanwhile, is typically used to extract thermodynamic parameters and assumes adsorption occurs on a heterogeneous surface [60]. Here, q_m reflects the adsorption capacity of a given layer, while KDR is a constant tied to adsorption energy. This isotherm also allows the average free energy of adsorption to be calculated, along with the energy required per adsorbed molecule, assuming unlimited transport of the pollutant to the adsorbent surface.

The Hill isotherm model describes a cooperative binding phenomenon, in which a ligand binds to one site on a macromolecule in a way that can influence binding at other sites on that same molecule. In this model, qH represents the adsorption capacity, nH is the Hill coefficient describing the binding interaction, and KH is the Hill constant.

Among the three-parameter isotherm models, the Redlich-Peterson model is commonly applied to liquid-phase adsorption of organic compounds. In this study, the Langmuir isotherm produced the highest R^2 among the two-parameter models, while the Redlich-Peterson model performed best among the three-parameter models. This suggests a more tightly packed adsorbent surface, with reduced influence from secondary factors on drug uptake.

Based on the findings, adsorption of the pharmaceutical contaminants onto the adsorbent follows a single-layer (monolayer) pattern, consistent with a homogeneous surface offering uniform adsorption energy. Since the β value in the Redlich-Peterson equation is close to 1, the Langmuir model provides a better fit to the experimental equilibrium data — a fit illustrated by the curve in Figure 10.

Table 3. Results of the Longmire and BET measurements of HCl-washed sludge

Model	Parameter	AMX
Langmuir isotherm	q_{max} $(mg.g^{-1})$	484.9
	K_L $(L.mg^{-1})$	0.012
	R^2	0.99
Freundlich isotherm	K_F $(mg^{1-n}.L^n.g^{-1})$	10.88
	n	1.393
	R^2	0.97
Temkin isotherm	B_T $(Kj.mol^{-1})$	64.22
	A_T $(L.mg^{-1})$	0.3175
	R^2	0.91
Redlich-Peterson	K_{RP} $(L.mg^{-1})$	4.842
	${}_{RP}\alpha_{(L.mg^{-1})}$	3.48×10^{-5}
	${}_{Rp}\beta$	2.261
	R^2	0.99
Hill isotherm	q_H $(mg.g^{-1})$	335.6
	K_H	111.8
	n_H	1.273
	R^2	0.99
Duinin-Radushkevich isotherm	q_{max} $(mg.g^{-1})$	235.9
	$K\times10^7(mol^2.kJ^2)$	1.076
	$E\times10^7$ $(kJ.mol^{-1})$	68.19
	R^2	.96

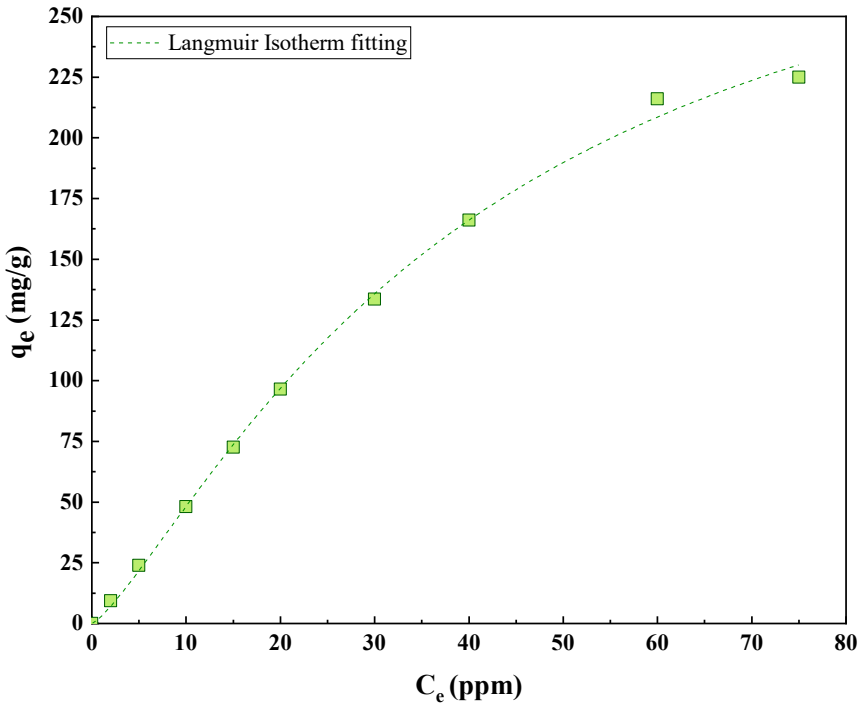


Figure 10. Curve fitting of Langmuir isotherm model for AMX adsorption (Initial concentration 2-75 mg/L, contact time 110 min, pH 6, adsorbent dose 1.4 mg/L and ambient temperature)

Effect of Temperature

As shown in Figure 11, rising temperature increases the kinetic energy of drug molecules in solution, giving them enough energy to be adsorbed onto the adsorbent surface — making adsorption more effective at higher temperatures. However, since adsorption capacity showed little sensitivity to temperature overall, and given the added energy cost of running experiments at elevated temperatures, 25°C was selected as the working temperature for this study [61].

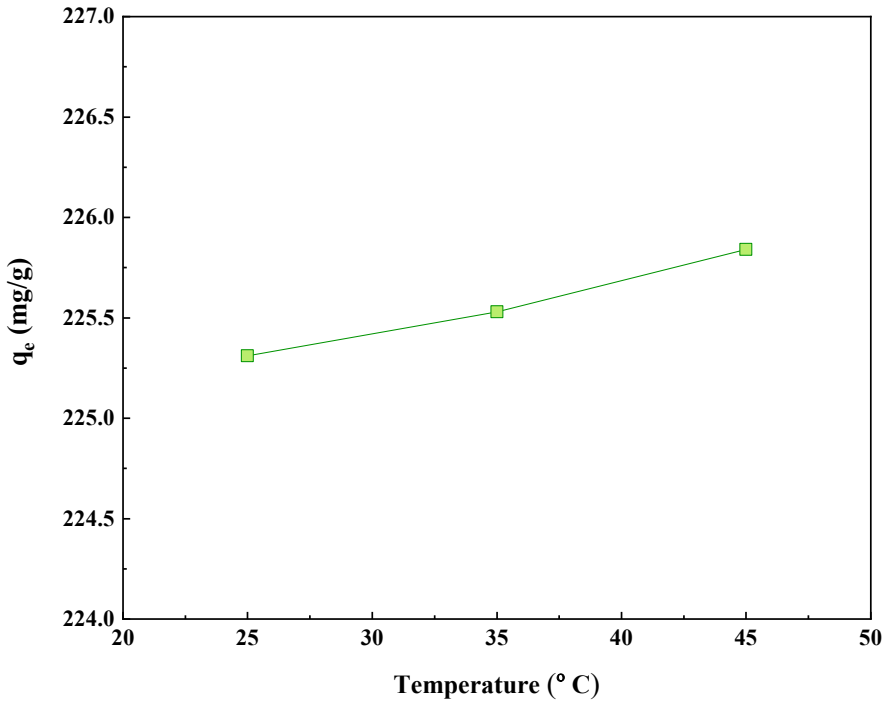


Figure 11. Effect of temperature on AMX adsorption rate under operating conditions (Initial concentration 75 mg/g, pH 6, adsorbent amount 1.4 g/L and contact time 110 min)

Adsorption Thermodynamics

Adsorption thermodynamics values (H, S, and G) were calculated using the van't Hoff equation as illustrated in Table 4. The negative enthalpy means the process is exothermic, and the positive entropy indicates an increase in disorder at the solid-solution boundary during the process, along with changes in the solid and adsorbate structures, which makes the process non-irreversible, whereas the negative Gibbs free energy indicates a spontaneous reaction. Adsorbent-pollutant interaction looks to be of physical adsorption in view of the magnitude of enthalpy, suggesting the adsorbent should be regenerable [62, 63].

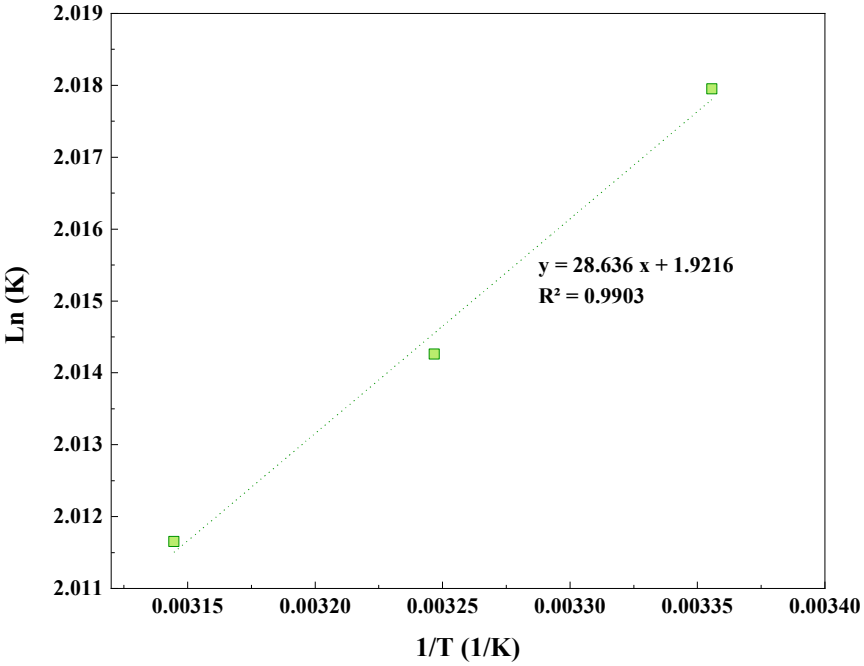


Figure 12. Van't-Hoff diagram of AMX adsorption

Table 4. Thermodynamic parameters of the adsorption process

Adsorbents	ΔS (J/mol/K)	ΔH (J/mol)	ΔG (KJ/mol) Temperature (K)		
			298	308	318
DWTS-HCl	15.976	-238.07	-4.998	-5.158	-5.318

Investigating the reusability of the adsorbent

Recovering the adsorbent for reuse is economically important. Although the price of metal-organic frameworks is higher than that of natural adsorbents and activated carbon, their very high adsorption capacity allows them to be used in smaller quantities, thereby providing greater economic value. According to Figure 7, the adsorbent can be used 6 times with a removal efficiency of 81.1%.

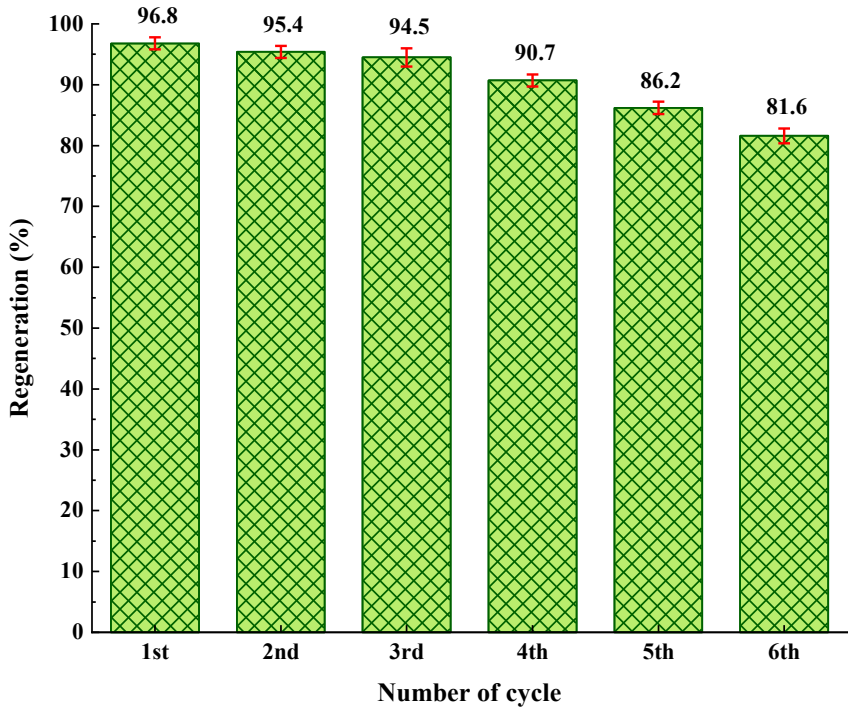


Figure 13. Absorbent recovery diagram with ethanol solvent

Effect of Ionic Strength on Adsorption Performance

As the concentration of sodium chloride (NaCl) in the solution increases, a noticeable decline in the adsorption capacity was observed. At high NaCl concentrations, sodium and chlorine ions act as competitors for the attachment of amoxicillin molecules to the adsorbent surface, at higher NaCl concentrations, sodium (Na^+) and chloride (Cl^-) ions competed with amoxicillin molecules for active adsorption sites on the adsorbent surface, resulting in reduced adsorption efficiency. reducing the adsorption capacity of the adsorbent. This phenomenon occurs due to the competition of ions at the adsorbent surface. Increasing the concentration of Na^+ and Cl^- ions can cause changes in the surface charge, which in turn affects the electrostatic forces between the adsorbent surface and amoxicillin. In other words, as the salt concentration increases, the effects of van der Waals and electrostatic forces decrease, and hence, amoxicillin will be less able to bind to the adsorbent surface. In general, at neutral pH, the surface charge is close to zero, causing the maximum adsorption capacity to be at concentrations lower than NaCl. However, with increasing NaCl concentration, negative effects on drug absorption such as amoxicillin are clearly observed, indicating competition between ions and changes in the surface properties of the adsorbent. This

clearly demonstrates the importance of investigating environmental conditions in the drug absorption process in aqueous systems.

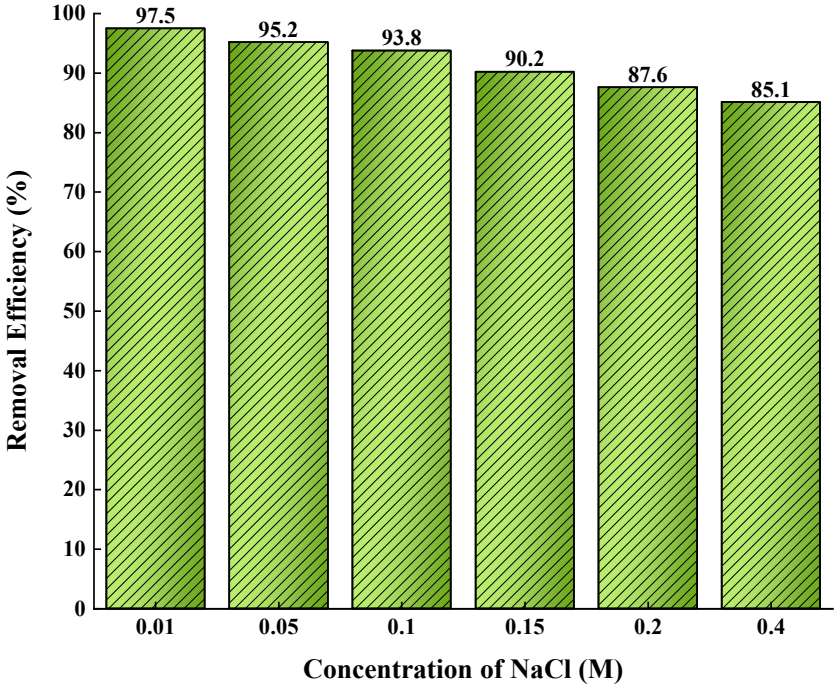


Figure 14. The effect of sodium chloride ionic strength on amoxicillin absorption.

Experimental Design

Preliminary experiments were first carried out to establish suitable ranges for pH, pollutant concentration, adsorbent dose, contact time, and temperature. Based on these ranges, the experimental design was developed in Design-Expert software (version 11) using response surface methodology (RSM) for statistical design, data analysis, and optimization. Specifically, a central composite design (CCD) was chosen as the RSM approach. The five main factors — pollutant concentration, adsorbent dose, contact time, and temperature — were each tested at five levels: -α (minimum), -1, 0 (central), +1, and +α (maximum), as outlined in Table 5.

Table 5. Variables and levels selected for experimental design using RSM and CCD design for AMX absorption

Factors	level		
	maximum (+1)	Zero central (0)	minimum (-1)
(A) Initial pH	9	6	3
(B) Contact time (min)	100	55	10
(C) Adsorbent dosage (g/L)	2	1.2	0.4
(D) Pollutant concentration (mg/L)	75	38.5	2
(E) Temperature (°C)	60	42.5	25

The total number of experiments with this method is $N = 2^K + 2K + n$, where k is the number of effective (main) factors in the process efficiency, which in this study was chosen to be 4. After determining the range of each parameter (Table 5), 46 experiments were designed in 1 block by the software. The experiments designed by the software were performed, and the percentage of drug removal was recorded.

Table 6. Experiments designed for AMX absorption with DX11 software

Std	Run	pH (A)	Time (B)	Dosage (C)	Concentration(D)	Temperature (E)
31	1	6	55	0.4	38.5	60
10	2	6	100	1.2	38.5	25
28	3	9	55	1.2	75	42.5
24	4	6	100	2	38.5	42.5
8	5	6	55	2	75	42.5
26	6	9	55	1.2	2	42.5
23	7	6	10	2	38.5	42.5
45	8	6	55	1.2	38.5	42.5
14	9	9	55	0.4	38.5	42.5
3	10	3	100	1.2	38.5	42.5
42	11	6	55	1.2	38.5	42.5
13	12	3	55	0.4	38.5	42.5
6	13	6	55	2	2	42.5
36	14	9	55	1.2	38.5	60
46	15	6	55	1.2	38.5	42.5
30	16	6	55	2	38.5	25
38	17	6	100	1.2	2	42.5
12	18	6	100	1.2	38.5	60
29	19	6	55	0.4	38.5	25
37	20	6	10	1.2	2	42.5
21	21	6	10	0.4	38.5	42.5
17	22	6	55	1.2	2	25

27	23	3	55	1.2	75	42.5
19	24	6	55	1.2	2	60
39	25	6	10	1.2	75	42.5
4	26	9	100	1.2	38.5	42.5
1	27	3	10	1.2	38.5	42.5
22	28	6	100	0.4	38.5	42.5
33	29	3	55	1.2	38.5	25
32	30	6	55	2	38.5	60
35	31	3	55	1.2	38.5	60
9	32	6	10	1.2	38.5	25
15	33	3	55	2	38.5	42.5
7	34	6	55	0.4	75	42.5
40	35	6	100	1.2	75	42.5
11	36	6	10	1.2	38.5	60
16	37	9	55	2	38.5	42.5
43	38	6	55	1.2	38.5	42.5
34	39	9	55	1.2	38.5	25
44	40	6	55	1.2	38.5	42.5
5	41	6	55	0.4	2	42.5
25	42	3	55	1.2	2	42.5
41	43	6	55	1.2	38.5	42.5
18	44	6	55	1.2	75	25
20	45	6	55	1.2	75	60
2	46	9	10	1.2	38.5	42.5

In this section, the simultaneous influence of other effective factors on the drug adsorption process was investigated using RSM in Design-Expert software. In this method, the five parameters considered were: pH (A), contact time (B), adsorbent amount (C), pollutant concentration (D), and temperature (E). The variables were predicted at five levels. Then, 46 experiments were designed in the form of 1 block, and the results are summarized in Table 6.

Table 7. Results of experiments designed using the response procedure method in the AMX adsorption process

Std	Run	pH (A)	Time (B)	Dosage (C)	Concentration (D)	Temperature (E)	Removal Efficiency (%)
31	1	6	55	0.4	38.5	60	58.4
10	2	6	100	1.2	38.5	25	73.4
28	3	9	55	1.2	75	42.5	42.3
24	4	6	100	2	38.5	42.5	91.3
8	5	6	55	2	75	42.5	68.5
26	6	9	55	1.2	2	42.5	30

23	7	6	10	2	38.5	42.5	62.1
45	8	6	55	1.2	38.5	42.5	78.5
14	9	9	55	0.4	38.5	42.5	34.2
3	10	3	100	1.2	38.5	42.5	75.4
42	11	6	55	1.2	38.5	42.5	86.5
13	12	3	55	0.4	38.5	42.5	44.9
6	13	6	55	2	2	42.5	54.7
36	14	9	55	1.2	38.5	60	30.6
46	15	6	55	1.2	38.5	42.5	79.5
30	16	6	55	2	38.5	25	55.3
38	17	6	100	1.2	2	42.5	85.7
12	18	6	100	1.2	38.5	60	95.9
29	19	6	55	0.4	38.5	25	49.8
37	20	6	10	1.2	2	42.5	56.7
21	21	6	10	0.4	38.5	42.5	59.6
17	22	6	55	1.2	2	25	45.2
27	23	3	55	1.2	75	42.5	61.3
19	24	6	55	1.2	2	60	59.3
39	25	6	10	1.2	75	42.5	68.4
4	26	9	100	1.2	38.5	42.5	56.1
1	27	3	10	1.2	38.5	42.5	42.9
22	28	6	100	0.4	38.5	42.5	77.3
33	29	3	55	1.2	38.5	25	32.5
32	30	6	55	2	38.5	60	59.2
35	31	3	55	1.2	38.5	60	61.8
9	32	6	10	1.2	38.5	25	60
15	33	3	55	2	38.5	42.5	50.6
7	34	6	55	0.4	75	42.5	62.4
40	35	6	100	1.2	75	42.5	94.3
11	36	6	10	1.2	38.5	60	61.1
16	37	9	55	2	38.5	42.5	35.8
43	38	6	55	1.2	38.5	42.5	80.2
34	39	9	55	1.2	38.5	25	37.5
44	40	6	55	1.2	38.5	42.5	78.6
5	41	6	55	0.4	2	42.5	58.2
25	42	3	55	1.2	2	42.5	38.9
41	43	6	55	1.2	38.5	42.5	87.2
18	44	6	55	1.2	75	25	68.6
20	45	6	55	1.2	75	60	70.2
2	46	9	10	1.2	38.5	42.5	39.8

Analysis of Variance (ANOVA)

ANOVA is a statistical technique, well known and commonly used for measuring the validity of the model. In the present research, the method of analysis of variance was employed for optimization of surface adsorption conditions of amoxicillin. Generally, ANOVA was carried out in the present study in accordance with CCD output results [64]. Table 7 outlines the ANOVA output table of surface adsorption of the drug. We are evaluating the degree and significance of independent parameters and their ranking based on their impact on the process based on two quantities: P value and F value. If we take into account that the test is performed at a 95% confidence level then from Table 7 we observe that F value of individual factors (listed from more to less influential ones) time, pollutant concentration, pH, temperature and finally the amount of adsorbent is in an order in which F value increase: 41236, 15183, 7509.3, 776.6, and 548.42, and for the sentence of lack of fit its P value and F value indicate that the generated models fit very well the experimental data by the software, another factor, indicating the quality of the model, is R2 that was calculated to be 0.98, it is near 1 that means it has small variation between predicted and actual data.

Table 8. Results of the analysis of variance model obtained for the AMX adsorption process

Source	Sum of Squares	df	Mean Square	F-value	p-value	Description
Model	14271.22	20	713.56	77.60	< 0.0001	significant
A- pH	650.25	1	650.25	70.72	< 0.0001	
B-Time (min)	2470.09	1	2470.09	268.63	< 0.0001	
C- Dosage (g/l)	66.83	1	66.83	7.27	0.0124	
D-Cons. (mg/l)	719.58	1	719.58	78.26	< 0.0001	
E- Temp. (˚C)	344.10	1	344.10	37.42	< 0.0001	
AB	65.61	1	65.61	7.14	0.0131	
AC	4.20	1	4.20	0.4570	0.5052	not significant
AD	25.50	1	25.50	2.77	0.1083	not significant
AE	327.61	1	327.61	35.63	< 0.0001	
BC	33.06	1	33.06	3.60	0.0695	not significant
BD	2.40	1	2.40	0.2613	0.6137	
BE	114.49	1	114.49	12.45	0.0016	
CD	23.04	1	23.04	2.51	0.1260	not significant
CE	5.52	1	5.52	0.6006	0.4456	not significant
DE	39.06	1	39.06	4.25	0.0498	
A^2	7571.33	1	7571.33	823.40	< 0.0001	
B^2	61.87	1	61.87	6.73	0.0156	
C^2	1287.46	1	1287.46	140.01	< 0.0001	
D^2	647.35	1	647.35	70.40	< 0.0001	
E^2	1350.03	1	1350.03	146.82	< 0.0001	

Residual	229.88	25	9.20			
Lack of Fit	149.66	20	7.48	0.4664	0.8981	not significant
Pure Error	80.21	5	16.04			
Cor Total	14501.10	45				
	R^2				0.9841	
	Adjusted R^2				0.9715	
	Predicted R^2				0.9508	
	Adeq Precision				31.87	
	C.V. %				4.98	

Analysis results

Empirical predictions were generated through least-squares regression, with Equation (1) used to estimate the response variable Y and evaluate the coefficients of the second-order model.

$$Y = \beta_0 + \sum \beta_i X_i + \sum \beta_{ii} X_i^2 + \sum \beta_{ij} X_i X_j + \varepsilon \quad (1)$$

In this equation, β0 denotes the constant term, βi the linear (independent) coefficients, βii the quadratic coefficients, βij the interaction coefficients, and ε the residual term accounting for experimental error. Positive coefficients in Equation (2) indicate a direct relationship with the response — that is, increasing the corresponding parameter leads to a higher response value. Negative coefficients, on the other hand, indicate an inverse relationship, where increasing the parameter reduces the response [65].

$$\begin{aligned}\text{Removal Efficiency} = {} & -216.7887 + 47.5237 \times \text{pH} - 0.0549 \times Time + 46.6742 \times Dosage \\ & + 0.9551 \times Cons. + 4.6667 \times Temp. - 0.0300 \times pH \times Time - 0.4270 \times pH \times Dosage \\ & - 0.0230 \times pH \times Cons. - 0.1723 \times pH \times Temp. + 0.0798 \times Time \times Cons. \\ & - 0.0004 \times Time \times Temp. + 0.0821 \times Dosage \times Cons. - 0.0839 \times Dosage \times Temp. \\ & - 0.0048 \times Cons. \times Temp. - 3.2726 \times pH^2 + 0.0013 \times Time^2 - 18.9778 \times Dosage^2 \\ & - 0.0064 \times Cons.^2 - 0.0406 \times Temp.^2\end{aligned} \quad (2)$$

Review of two-dimensional and three-dimensional graphs

To visualize how different parameters interact and jointly influence the response, this section uses both two- and three-dimensional plots, which make it easier to interpret the combined effect of two factors on the response variable. In the 3D plots, contour lines trace out a range of response

values, while the corresponding 2D contour plots highlight regions of better performance — that is, higher amoxicillin removal efficiency — with darker shading indicating greater efficiency.

Effect of pH and contact time on AMX surface adsorption

Figure 8 shows the parallel line diagram of the effect of the two factors, pH and contact time. According to this diagram, removal efficiency increases with pH up to an optimum point and then decreases. This is due to the effect of electrostatic forces. Considering the isoelectric point of the adsorbent, which is equal to 6, at pH values below that, the adsorbent surface is positive. At pH values above it, the adsorbent's surface charge is negative. For drugs, at pH values below the pKa, the drug's surface charge is positive, and at pH values above the pKa, it is negative. As pH increases, the surface charges of the adsorbent and the drug are the same, and electrostatic repulsion reduces drug removal efficiency [59]. At a fixed pH, increasing contact time enhances adsorption efficiency by increasing the interaction time [66].

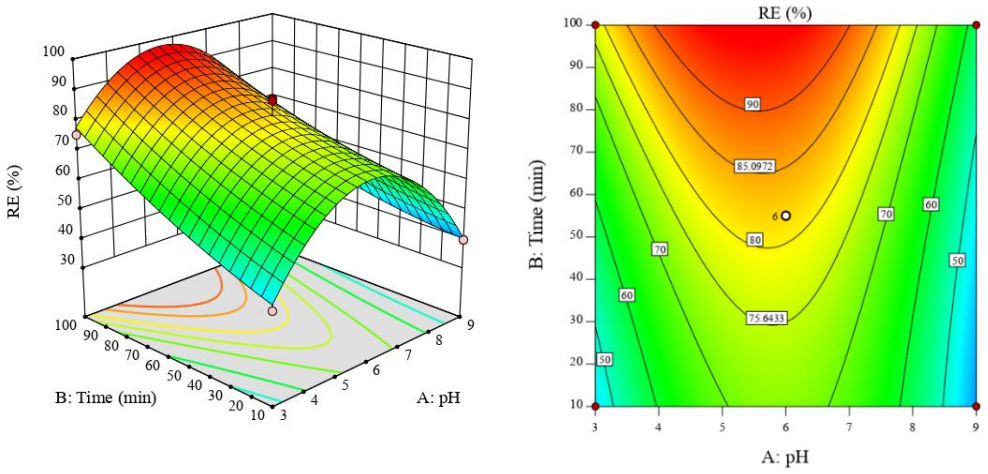


Figure 15. Two-dimensional and three-dimensional diagrams investigating the simultaneous effect of pH and contact time on the AMX adsorption process

Simultaneous effect of pH and temperature on AMX adsorption

Figure 9 illustrates the combined effect of pH and temperature. According to this graph, at constant pH, with increasing temperature up to 45 ° C, the removal efficiency increases. However, with increasing temperature from 45 to 60 ° C, the removal efficiency decreases due to the high movement of molecules and also the repulsion between the adsorbent and the pollutant [67]. At

constant temperature, due to the effect of electrostatic forces and the surface charge of the pollutant, the removal efficiency first increases and then decreases [61].

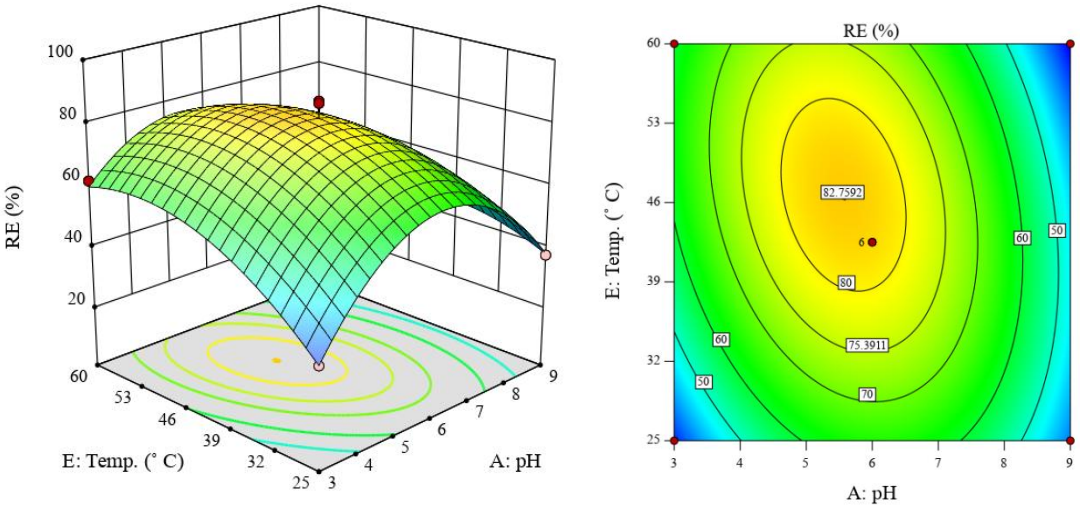


Figure 16. Two-dimensional and three-dimensional diagrams investigating the simultaneous effect of pH and temperature on the AMX adsorption process

Effect of Contaminant Concentration and Contact Time

Figure 10 shows the parallel-line diagram of the effects of two factors: contact time and pollutant concentration. At a constant time, the pollutant concentration increases to 60 ppm. Then, due to saturation of the adsorbent surface with the pollutant, the removal efficiency reaches a constant equilibrium value. The driving force for the mass transfer process is the increase in collisions of molecules and surfaces. With an increase in molecular concentration, the probability of collisions between molecules and the adsorbent surface increases, thereby increasing mass transfer from the solution phase to the solid phase. An increase in the number of collisions causes molecules to move away from the solution phase [68]. According to this diagram, at a constant pollutant concentration, removal efficiency increases with increasing contact time. In the initial moments, the surface available for drug adsorption by the adsorbent is very large. As a result, the adsorption rate increases, leading to rapid drug absorption. At the moment of equilibrium, the rates of adsorption and desorption are equal, so the rate of adsorption at equilibrium will be zero. At the moment the

adsorbent reaches equilibrium, the removal efficiency will not increase significantly with time [66].

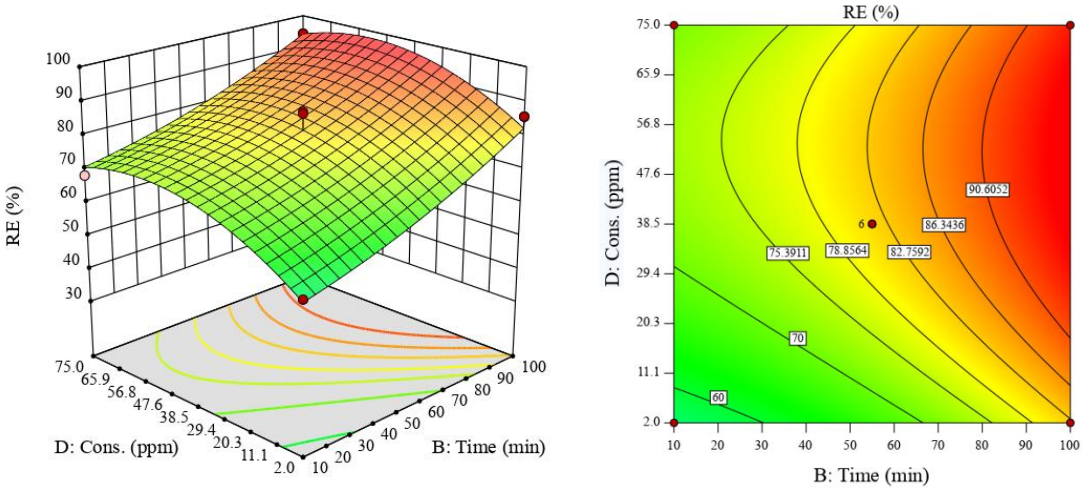


Figure 17. Two-dimensional and three-dimensional diagrams investigating the simultaneous effect of pollutant concentration and contact time on the AMX adsorption process

Effect of Adsorbent Dose and Contaminant Concentration

As shown in Figure 11, the line graph depicts the effects of two factors: adsorbent amount and drug concentration. According to this graph, at a constant drug concentration, the removal efficiency first increases and then decreases with increasing adsorbent amount. This is because increasing the adsorbent mass leads to adhesion and clumping within the adsorbent. With clumping, the available adsorption surface area decreases, reducing removal efficiency. On the other hand, a low adsorbent dose below the optimal level also reduces drug removal efficiency. The reason is that a low amount of adsorbent is encountered at a very high amount of drug at a moment, causing the adsorbent to be saturated at the first moment and, so to speak, poisoned [69].

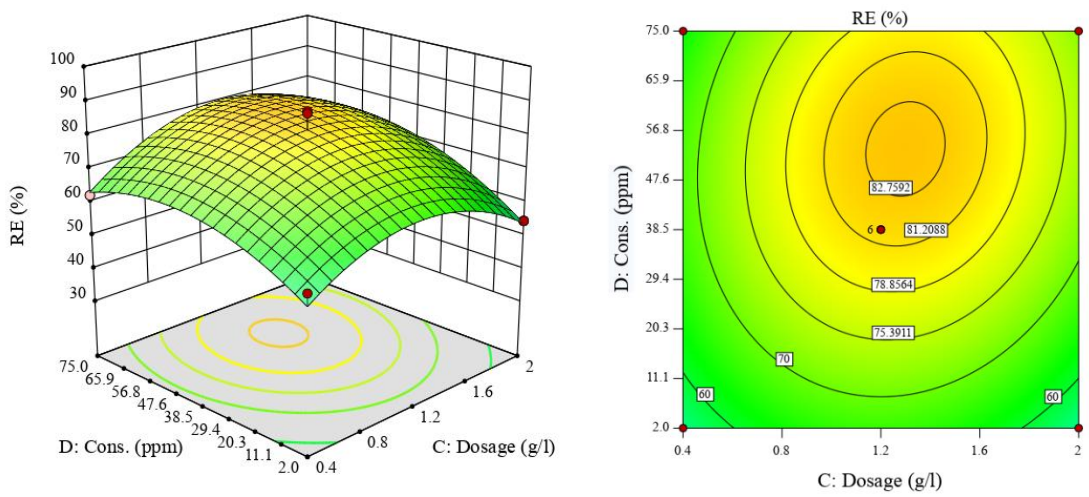


Figure 18. Two-dimensional and three-dimensional diagrams investigating the simultaneous effect of pollutant concentration and adsorbent amount on the AMX adsorption process

Effect of Contaminant Concentration and Temperature

Figure 12 shows that, at a constant drug concentration, the removal efficiency increases with increasing temperature up to 45 °C due to higher molecular energy. However, as the temperature increases from 45 to 60 °C, the removal efficiency decreases due to the weakening of intermolecular forces. At a constant temperature, with increasing drug concentration, the removal rate first increases and then decreases. In surface adsorption, as drug concentration increases, the adsorption rate initially increases due to the availability of vacant adsorbent surface sites. As surface saturation approaches, the adsorption rate decreases because the number of vacant sites decreases. At very high concentrations, the accumulation of adsorbed molecules and competition among them reduce adsorption efficiency. Thus, at constant temperature, the drug adsorption behavior first increases and then decreases.

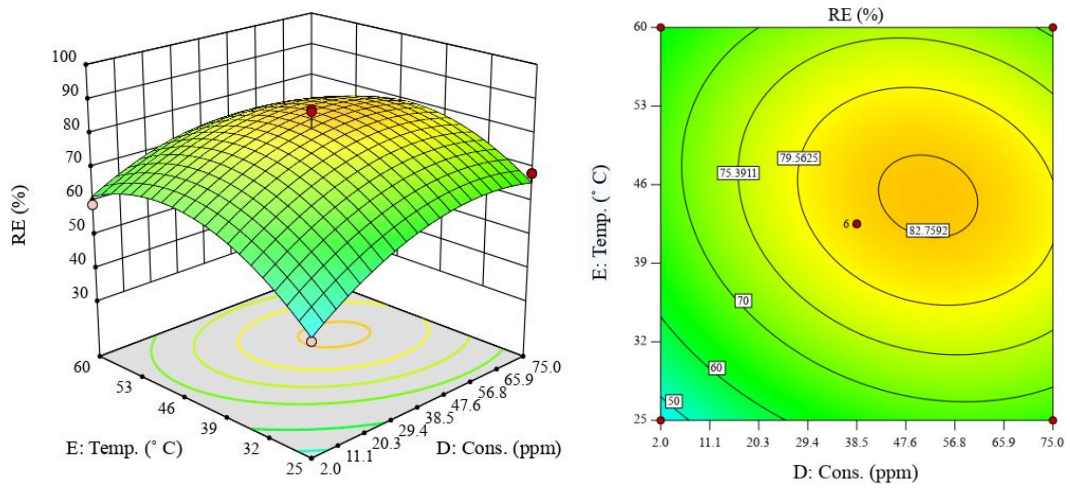


Figure 19. Two-dimensional and three-dimensional diagrams investigating the simultaneous effect of temperature and pollutant concentration on the AMX adsorption process

Evaluation of optimal conditions and accuracy of the predicted model

One key benefit of an experimental design approach to adsorption studies is that it allows optimal operating conditions to be systematically identified. What counts as "optimal," however, depends on the priorities at hand — for instance, maximizing removal efficiency, reaching a target efficiency as quickly as possible to save energy, minimizing adsorbent use to cut costs, or avoiding extreme pH conditions to limit environmental impact. All of these considerations can shape how optimal conditions are defined and selected. Such conditions can be modeled using software, and close agreement between the software's predictions and the experimental results provides validation of the model. In this study, two optimal points were identified. The first spans the full range of tested factor levels, while the second specifically targets the highest possible drug removal rate. Both sets of conditions were then used to evaluate the adsorbent's repeatability and overall efficiency.

Table 9. Optimal responses for the AMX adsorption process

Defined relationship for features in software	pH (± 0.05)	Contact time (min) (± 1)	Absorbent Amount (g/l) (± 0.03)	AMX concentration (ppm) (± 1)	Temperature (˚C) (± 1)	Removal efficiency based on prediction (± 1.5)	Removal efficiency based on experimental results (%) (± 1.5)
All characteristics within the range of selected levels	7.4	87.6	1.3	65.82	40.42	79.84	77.58
The removal efficiency should be the highest	6	100	1.4	75	40	94.07	95

Conclusion

A cost-effective adsorbent was developed from activated sludge processed under various conditions, and characterization results confirmed its potential as an effective material for removing AMX residues from water. AMX concentration in the solution was measured to evaluate adsorptive capacity, and the process was optimized, resulting in optimal parameters including contact time, pH 6, adsorbent dose 1.4 g/L, and initial AMX concentration 75 mg/L. The application of hydrochloric acid-activated (0.5 M) sludge also fitted well with the Langmuir model. The adsorption behavior of the chemically activated adsorbent also performed well over 6 reuse cycles. These findings suggest that sludge readily available from water treatment plants could, with minor modifications, serve as an efficient, low-cost adsorbent for AMX removal at both pilot and industrial scales.

Acknowledgements

The Department of Water and Wastewater Research Center, Water Research Institute, Tehran, Iran.

Author Contributions

FH contributed to the conceptualization, monitoring the project, and investigation. MA contributed to writing and editing the manuscript, analyzing data, and investigation. SHD and AMN contributed to the experimental section. All authors gave their approval for publication.

Funding statement

This work was supported by the National Water and Wastewater Engineering Company of Iran (NWWEC), Tehran, Iran.

Data availability

All data generated/analyzed during this study are included in this published article and are publicly available.

References:

1. Shumiye, E., et al., *Preparation of an activated adsorbent from water treatment plant sludge for phosphate removal from wastewater: optimization, characterization, isotherm, and kinetics studies.* Journal of Water, Sanitation and Hygiene for Development, 2024. **14**(2): p. 122-143.
2. Lin, L., H. Yang, and X. Xu, *Effects of water pollution on human health and disease heterogeneity: a review.* Frontiers in environmental science, 2022. **10**: p. 880246.
3. Scanlon, B.R., et al., *Global water resources and the role of groundwater in a resilient water future.* Nature Reviews Earth & Environment, 2023. **4**(2): p. 87-101.
4. Zaidi, N., et al., *Pharmaceuticals and personal care products as emerging contaminants: environmental fate, detection, and mitigation strategies.* International Journal of Environmental Analytical Chemistry, 2025: p. 1-29.
5. Rukhsar, A., et al., *Chitosan-based adsorbents and catalysts for removal of toxic pollutants from water and wastewater.* Topics in Catalysis, 2025. **68**(9): p. 893-915.
6. Aziz, K., et al., *Recent advances in nanomaterial-based adsorbents for removal of pharmaceutical pollutants from wastewater.* Materials Horizons, 2025.
7. Sousa, P.M., et al., *Microalgae for microplastic removal from water and wastewater: a review.* Environmental Chemistry Letters, 2025. **23**(2): p. 611-648.
8. Fan, Y., et al., *Treatment of Livestock and Poultry Breeding Wastewater by Multistage Series System: Pollutant Removal Efficiency and Mechanism.* Water, Air, & Soil Pollution, 2025. **236**(4): p. 1-12.
9. Liu, G., et al., *A review on the industrial waste based adsorbents for the removal of pollutants from water: Modification methods and adsorption study.* Resources, Environment and Sustainability, 2024: p. 100183.
10. Sarizadeh, G., et al., *Efficiency of hospital wastewater treatment system in removal of level of toxic, microbial, and organic pollutant.* Toxin Reviews, 2022. **41**(3): p. 721-730.
11. Samrot, A.V., et al., *Sources of antibiotic contamination in wastewater and approaches to their removal—An overview.* Sustainability, 2023. **15**(16): p. 12639.
12. Domínguez-Montero, L., et al., *Working Toward an Environmental Risk Assessment of Emerging Contaminants in Wastewater: the Case of Amoxicillin.* Water, Air, & Soil Pollution, 2025. **236**(6): p. 366.
13. Kushwaha, S.P., et al., *Human health hazards due to antimicrobial resistance spread*, in *Antimicrobial resistance in wastewater and human health*. 2023, Elsevier. p. 225-240.
14. Zhang, Z., et al., *Assessment of global health risk of antibiotic resistance genes.* Nature communications, 2022. **13**(1): p. 1553.
15. Larsson, D.J. and C.-F. Flach, *Antibiotic resistance in the environment.* Nature Reviews Microbiology, 2022. **20**(5): p. 257-269.
16. Hanna, N., A.J. Tamhankar, and C.S. Lundborg, *Antibiotic concentrations and antibiotic resistance in aquatic environments of the WHO Western Pacific and South-East Asia regions: a systematic review and probabilistic environmental hazard assessment.* The Lancet Planetary Health, 2023. **7**(1): p. e45-e54.
17. Sangamnere, R., et al., *A critical review of conventional and emerging wastewater treatment technologies.* Sustainable Water Resources Management, 2023. **9**(2): p. 58.
18. Shamshad, J. and R.U. Rehman, *Innovative approaches to sustainable wastewater treatment: a comprehensive exploration of conventional and emerging technologies.* Environmental Science: Advances, 2025.
19. Ayach, J., et al., *Comparing conventional and advanced approaches for heavy metal removal in wastewater treatment: an in-depth review emphasizing filter-based strategies.* Polymers, 2024. **16**(14): p. 1959.
20. Rodríguez, C., et al., *Water context in Latin America and the Caribbean: distribution, regulations and prospects for water reuse and reclamation.* Water, 2022. **14**(21): p. 3589.

21. Silva-Rodríguez de San Miguel, J.A., *Water management in Europe and Latin America.* Management of Environmental Quality: An International Journal, 2018. **29**(2): p. 348-367.
22. Zhou, X., et al., *Occurrence of typical antibiotics, representative antibiotic-resistant bacteria, and genes in fresh and stored source-separated human urine.* Environment international, 2021. **146**: p. 106280.
23. Aguilar-Rangel, E.J., et al., *Hospital Wastewater as a Reservoir of Contaminants of Emerging Concern: A Study Report from South America, Chile.* Antibiotics, 2025. **14**(11): p. 1111.
24. Elizalde-Velázquez, A., et al., *Amoxicillin in the aquatic environment, its fate and environmental risk*, in *Environmental health risk-hazardous factors to living species*. 2016, IntechOpen.
25. Okoye, C.O., et al., *Antibiotic resistance in the aquatic environment: analytical techniques and interactive impact of emerging contaminants.* Environmental Toxicology and Pharmacology, 2022. **96**: p. 103995.
26. Imran, M., et al., *Nanostructured material-based optical and electrochemical detection of amoxicillin antibiotic.* Luminescence, 2023. **38**(7): p. 1064-1086.
27. Grumezescu, A.M., et al., *Biocompatible Fe3O4 increases the efficacy of amoxicillin delivery against Gram-positive and Gram-negative bacteria.* Molecules, 2014. **19**(4): p. 5013-5027.
28. Subhadarshini, A., et al., *ZIF-8 based magnetic MOF nanocomposite: A dual functional material for amoxicillin degradation and bacteria elimination.* Journal of Molecular Structure, 2025: p. 143702.
29. Felis, E., et al., *Antimicrobial pharmaceuticals in the aquatic environment-occurrence and environmental implications.* European Journal of Pharmacology, 2020. **866**: p. 172813.
30. Georgin, J., et al., *Main advances and future prospects in the remediation of the antibiotic amoxicillin with a focus on adsorption technology: A critical review.* Journal of water process engineering, 2023. **56**: p. 104407.
31. Laksaci, H., et al., *Elimination of amoxicillin by adsorption on coffee waste based activated carbon.* Journal of Molecular Structure, 2023. **1274**: p. 134500.
32. Barbooti, M.M. and S.H. Zahraw, *Removal of amoxicillin from water by adsorption on water treatment residues.* Baghdad Science Journal, 2020. **17**(3): p. 48.
33. Caravaca, M., et al., *Total removal of amoxicillin from water using magnetic core nanoparticles functionalized with silver.* Environmental Research, 2022. **211**: p. 113091.
34. Rezaei, J., et al., *Evaluation of membrane bioreactor-hollow fiber (MBR-HF) pilot performance in the treatment of wastewater facing with different concentrations of amoxicillin (AMX) as shock loads.* Journal of Environmental Chemical Engineering, 2020. **8**(4): p. 103944.
35. Muduli, M., et al., *Assessment of amoxicillin (AMX) removal from aqueous medium through Rhapis-based bioretention system.* Environmental Science and Pollution Research, 2024. **31**(49): p. 59071-59086.
36. Silva, B.S., et al., *Removal of amoxicillin from processing wastewater by ozonation and UV-aided ozonation: kinetic and economic comparative study.* Water, 2022. **14**(20): p. 3198.
37. Roushree, R. and R. Haimbodi, *Recent advances in ZnO-based nanocomposites for amoxicillin photocatalytic degradation and adsorption in wastewater: a review.* Journal of Inorganic and Organometallic Polymers and Materials, 2025: p. 1-38.
38. Mohammed, A.K., et al., *Removal of amoxicillin from contaminated water using modified bentonite as a reactive material.* Heliyon, 2024. **10**(3).
39. Yavari, K., et al., *Removal of amoxicillin from hospital waste using Fe2O3-Ag adsorbent and optimization by response surface methodology and machine learning prediction.* Current Research in Green and Sustainable Chemistry, 2025: p. 100483.
40. Ochoa-Munoz, Y.H., et al., *Rice husk-derived silica aerogels for efficient removal of amoxicillin and erythromycin from water.* Surfaces and Interfaces, 2025: p. 108089.
41. Şahin, M., M. Mısır, and Y. Arslan, *Removal of Amoxicillin Using a New Adsorbent: Silver Nanoparticle Modified With Poly (ε-Caprolactone)-Block-Poly (L-Lactide) Copolymer.* Journal of Applied Polymer Science, 2025. **142**(10): p. e56556.

42. Dolfini, N., C.M.B.d. Araujo, and N.C. Pereira, *Amoxicillin removal from water by adsorption on activated carbon of mineral sources: discussion of experimental data, mechanisms and modeling.* Environmental Technology, 2024. **45**(8): p. 1636-1650.
43. Liu, X., et al., *Removal of amoxicillin from water by concrete-based hydrotalcites: Efficiency and mechanism.* Process Safety and Environmental Protection, 2022. **163**: p. 210-217.
44. Shamim, M.A., et al., *Metal organic frameworks (MOFs) as a cutting-edge tool for the selective detection and rapid removal of heavy metal ions from water: Recent progress.* Journal of Environmental Chemical Engineering, 2022. **10**(1): p. 106991.
45. Hosny, N.M., I. Gomaa, and M.G. Elmahgary, *Adsorption of polluted dyes from water by transition metal oxides: A review.* Applied Surface Science Advances, 2023. **15**: p. 100395.
46. Li, N., et al., *A novel cellulose/lignin/montmorillonite ternary hybrid aerogel for efficiently adsorptive removal of antibiotics from water.* Chemical Engineering Journal, 2023. **466**: p. 143265.
47. Eniola, J.O., et al., *Application of conventional and emerging low-cost adsorbents as sustainable materials for removal of contaminants from water.* Environmental Science and Pollution Research, 2023. **30**(38): p. 88245-88271.
48. El Mahdaoui, A., et al., *Progress in the modification of cellulose-based adsorbents for the removal of toxic heavy metal ions.* Journal of Environmental Chemical Engineering, 2024. **12**(5): p. 113870.
49. Gulhan, H., et al., *Use of water treatment plant sludge in high-rate activated sludge systems: A techno-economic investigation.* Science of The Total Environment, 2023. **901**: p. 166431.
50. Escamilla-García, P.E., *Landfills in developing economies: drivers, challenges, and sustainable solutions*, in *Technical Landfills and Waste Management: Volume 1: Landfill Impacts, Characterization and Valorisation*. 2024, Springer. p. 157-170.
51. Barzigar, A., S. Hosseinalipour, and A. Pani, *The critical role of dewatering and drying science and technology in waste management.* Drying Technology, 2026. **44**(2): p. 135-137.
52. Taron, A., et al., *Sewage sludge: a review of business models for resource recovery and reuse.* 2023.
53. Sharma, S. and M.M. Ahammed, *Use of recovered coagulant from water treatment sludge for greywater treatment.* Environmental Science and Pollution Research, 2025. **32**(30): p. 18209-18225.
54. Mosaferi, M., et al., *A comprehensive review of cyclic activated sludge processes in wastewater treatment: Current perspectives and future challenges.* Sustainable Chemistry for the Environment, 2024: p. 100191.
55. Kang, X., et al., *Removal of amoxicillin from aqueous solution using sludge-based activated carbon modified by walnut shell and nano-titanium dioxide.* Water Reuse, 2021. **11**(1): p. 97-109.
56. Ali, A., Y.W. Chiang, and R.M. Santos, *X-ray diffraction techniques for mineral characterization: A review for engineers of the fundamentals, applications, and research directions.* Minerals, 2022. **12**(2): p. 205.
57. Cristiano, E., et al., *A comparison of point of zero charge measurement methodology.* Clays and Clay Minerals, 2011. **59**(2): p. 107-115.
58. Emami, N., et al., *Adsorption of cefixime and lamotrigine on HKUST-1/ZIF-8 nanocomposite: isotherms, kinetics models and mechanism.* International Journal of Environmental Science and Technology, 2023. **20**(2): p. 1645-1672.
59. Langmuir, I., *The constitution and fundamental properties of solids and liquids. Part I. Solids.* Journal of the American chemical society, 1916. **38**(11): p. 2221-2295.
60. Temkin, M., *Kinetics of ammonia synthesis on promoted iron catalysts.* Acta physiochim. URSS, 1940. **12**: p. 327-356.
61. Ariannezhad, M., et al., *The nano-magnetite-loaded 2-mercaptobenzoxazole as an adsorbent for the selective removal of the Pb2+, Ni2+ and Cd2+ ions from aqueous solutions.* Korean Journal of Chemical Engineering, 2021. **38**(7): p. 1510-1521.
62. Lima, E.C., et al., *A critical review of the estimation of the thermodynamic parameters on adsorption equilibria. Wrong use of equilibrium constant in the Van't Hoof equation for calculation of thermodynamic parameters of adsorption.* Journal of molecular liquids, 2019. **273**: p. 425-434.

63. Han, R., et al., *Study of equilibrium, kinetic and thermodynamic parameters about methylene blue adsorption onto natural zeolite.* Chemical Engineering Journal, 2009. **145**(3): p. 496-504.
64. Hosmer Jr, D.W., S. Lemeshow, and R.X. Sturdivant, *Applied logistic regression*. 2013: John Wiley & Sons.
65. Derikvandi, H., M. Vosough, and A. Nezamzadeh-Ejhieh, *A novel double Ag@ AgCl/Cu@ Cu2O plasmonic nanostructure: experimental design and LC-Mass detection of tetracycline degradation intermediates.* International Journal of Hydrogen Energy, 2021. **46**(2): p. 2049-2064.
66. Kurniawati, D., et al. *Effect of contact time adsorption of rhodamine B, methyl orange and methylene blue colours on langsat shell with batch methods*. in *Journal of Physics: Conference Series*. 2021. IOP Publishing.
67. Najafipour, I., et al., *Synthesis of Fe3O4@ MIL-101-OH/Chitosan for adsorption and release of doxorubicin.* Polymer Testing, 2025. **142**: p. 108659.
68. Basu, S., G. Ghosh, and S. Saha, *Adsorption characteristics of phosphoric acid induced activation of bio-carbon: Equilibrium, kinetics, thermodynamics and batch adsorber design.* Process Safety and Environmental Protection, 2018. **117**: p. 125-142.
69. Nasseh, I., et al., *Metronidazole removal methods from aquatic media: a systematic.* Ann Milit. Health Sci. Res, 2016. **14**: p. e13756.